Interactions between Global SST Anomalies and the Midlatitude Atmospheric Circulation

Ngar-Cheung Lau
Geophysical Fluid Dynamics Laboratory, NOAA, Princeton University, Princeton, New Jersey

ABSTRACT

A review is given of the processes contributing to variability of the atmosphere–ocean system on interannual timescales. Particular emphasis is placed on the relationships between midlatitude atmospheric fluctuations and sea surface temperature (SST) anomalies in various geographical sites. Various hypotheses are tested using output from a coordinated set of general circulation model experiments, which are subjected to time-varying SST forcing observed during 1946–88 in different parts of the world's oceans. It is demonstrated that tropical Pacific SST fluctuations associated with El Niño–Southern Oscillation (ENSO) episodes produce a strong extratropical response in the model atmosphere, whereas the atmospheric signal associated with midlatitude SST anomalies is less robust. Analysis of a 100-yr control experiment, which is conducted in the absence of any interannual SST forcing, indicates that a substantial fraction of the simulated atmospheric variability may be attributed to internal dynamical processes alone.

The observed coexistence of tropical ENSO events with SST anomalies in the extratropical North Pacific is successfully reproduced by forcing the model atmosphere with tropical Pacific SST variations and allowing the atmospheric perturbations thus generated to drive a simple ocean mixed layer model inserted at ocean grid points outside the tropical Pacific. This simulation affirms the role of the atmospheric circulation as a "bridge" linking SST changes in different parts of the world's oceans. The midlatitude model responses in the presence of local air–sea interactions are noticeably stronger than the corresponding responses without such interactions. This finding is indicative of the positive feedback processes inherent in extratropical air–sea coupling.

1. Introduction

On account of the large thermal capacity of seawater and the slowly varying oceanic currents, the surface conditions of the world's oceans typically fluctuate on timescales that are much longer than those of the atmosphere. Meteorologists have long regarded the surface properties of the oceans (in particular, sea surface temperature, or SST) as a prime candidate for inciting low-frequency atmospheric changes. Considerable efforts have been expended to delineate the influence of air–sea interactions on atmospheric variability at different geographical sites. It is now generally recognized that the linkage between oceanic and atmospheric fluctuations is not only an important building block for constructing a comprehensive knowledge base of the climate system, but also has far-reaching practical implications, particularly in the realm of extended-range prediction of weather and climate.

In this article, we offer a brief survey of the recent advances in our understanding of the relationships between SST anomalies and the atmospheric circulation in various locations. We shall focus on meteorological variations *in the midlatitudes* and evaluate different scenarios linking atmospheric responses to forcing by local or remote SST changes. The pathways through which the air–sea coupling acts in the opposite direction, that is, with the atmosphere driving the ocean, are also explored. For the sake of uniformity and organizational simplicity, the main themes will

Corresponding author address: Dr. Ngar-Cheung Lau, Geophysical Fluid Dynamics Laboratory, NOAA, Princeton University, P.O. Box 308, Princeton, NJ 08542.
E-mail: gl@gfdl.gov
In final form 12 July 1996.

be illustrated by drawing results from a single source, namely, output of a suite of experiments conducted in recent years at the Geophysical Fluid Dynamics Laboratory (GFDL) with a general circulation model.

2. Worldwide SST anomalies and concomitant atmospheric changes in the northern extratropics

The best-known mode of SST variability on interannual timescales is perhaps that associated with the El Niño–Southern Oscillation (ENSO) phenomenon in the tropical Pacific. The temporal variations of the observed SST field in the equatorial central and eastern Pacific during the northern winters of the 1946–88 period are depicted in Fig. 1b. It is seen that the observational record is interspersed with warm (or El Niño) and cold (or La Niña) episodes. With the exception of the decade-long warm spell after 1976, the typical lifetime of these ENSO cycles is several years.

Analyses performed by Weare et al. (1976), Hsiung and Newell (1983), Nitta and Yamada (1989), Pan and Oort (1990), and Folland and Parker (1990) of the observed data on a global basis reveal that the SST changes noted above are not confined to the tropical Pacific, but are instead correlated with a global-scale pattern having centers of action in the tropical Indian and Atlantic Oceans, as well as in the extratropical waters. Of special interest are the simultaneous SST fluctuations in the central subtropical North Pacific. In Fig. 1a the time series of wintertime SST anomalies averaged over the latter region is shown. Comparison between the two panels in Fig. 1 indicates that the polarity of SST anomalies in the central North Pacific tends to be opposite to that in the ENSO region. It is particularly noteworthy that the prominent warm SST anomalies observed in the tropical Pacific during the El Niño winters of 1957/58, 1969/70, 1972/73, 1976/77, 1982/83, 1986/87, and 1987/88 are coincident with pronounced cold anomalies in the central North Pacific. We shall henceforth refer to this set of seven winters as the "WTP/CNP" (an abbreviation of "warm tropical Pacific/cold North Pacific") winters. Conversely, the outstanding La Niña winters of 1949/50, 1955/56, 1964/65, 1967/68, 1970/71, 1973/74, and 1975/76, when cold tropical Pacific SST coexists with warm North Pacific waters, will be denoted as the "CTP/WNP" winters. Throughout this paper, we shall present data patterns obtained by subtracting the average of a given field over the CTP/WNP winters from the corresponding average over the WTP/CNP winters. These patterns will hereafter be referred to as the "WTP/CNP–CTP/WNP composites."

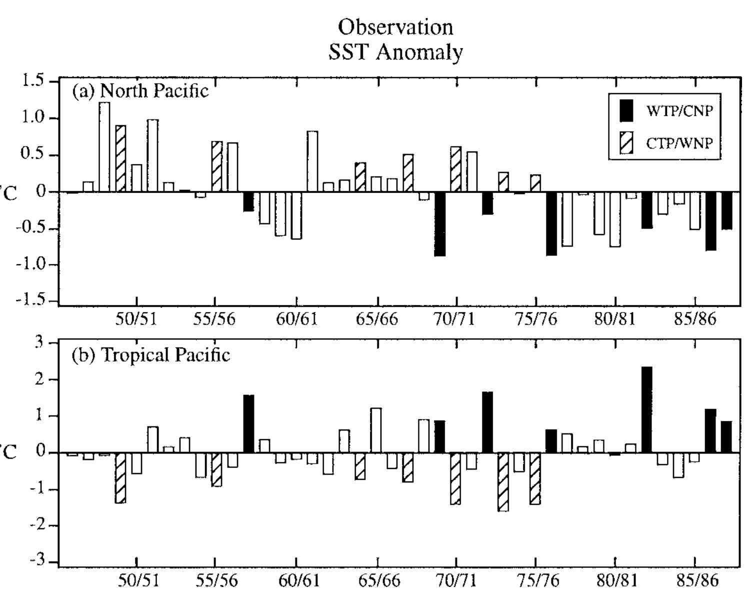

FIG. 1. Time series of the observed SST anomalies during the northern winter in the (a) North Pacific region between 27° and 45°N, 170°E and 146°W, and (b) tropical Pacific region between 5°S and 5°N, 180° and 90°W. Winters highlighted by black columns indicate outstanding events of warm tropical Pacific/cold North Pacific (WTP/CNP) temperatures. Winters highlighted by striped columns indicate outstanding events of cold tropical Pacific/warm North Pacific (CTP/WNP) temperatures. Note that the range of the ordinate in (a) is half of that in (b). Throughout this paper, the northern winter season is defined as the 3-month period from December to February.

The WTP/CNP–CTP/WNP composite for the observed near-global SST field is displayed in Fig. 2b. This pattern offers a clear depiction of the worldwide SST changes accompanying ENSO episodes in the tropical Pacific. Warm anomalies in the latter region are seen to occur in conjunction with prominent warm anomalies in the Indian Ocean, the Caribbean region, and the North Pacific waters off the west coast of North America, as well as with cold anomalies in the central North Pacific, the Gulf of Mexico/Bermuda region, and parts of the South Pacific. The polarity of the SST anomalies in various sites is reversed during cold periods in the tropical Pacific.

The atmospheric circulation anomaly in the northern extratropics associated with the global SST pattern described above is illustrated in Fig. 2a, which shows the WTP/CNP–CTP/WNP composite of the observed 500-hPa height field. The principal centers of action in the atmosphere are located in the North Pacific/North American sector. WTP/CNP winters are seen to coincide with above normal heights in the subtropical North Pacific and western Canada, and below-normal heights over the midlatitude North Pacific and southeastern United States. The coexistence of this characteristic atmospheric flow pattern with SST anomalies at various sites has been thoroughly documented in many observational studies, including those of Namias (1969), Horel and Wallace (1981), and van Loon and Madden (1981).

The empirical evidence presented in Fig. 2 poses two immediate questions.

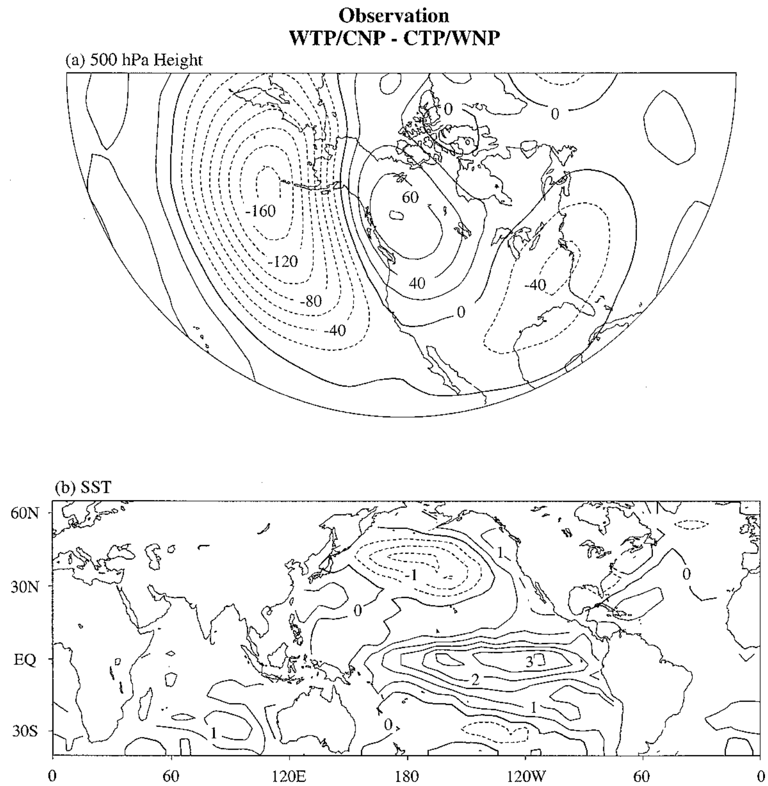

FIG. 2. Composite patterns obtained by subtracting the average over the seven CTP/WNP winters from the average over the seven WTP/CNP winters (see highlighted columns in Fig. 1), for observed (a) 500-hPa height, contour interval: 20 m; and (b) SST, contour interval: 0.5°C.

- Among the various SST anomaly centers highlighted in Fig. 2b, which site (or sites) is particularly effective in forcing the atmospheric pattern shown in Fig. 2a?
- Why are ENSO-related SST anomalies in the tropical Pacific so well correlated with oceanic changes elsewhere in the world's oceans?

3. Contending hypotheses

Notions on the origin of recurrent anomalous structures in the extratropical atmospheric circulation, such as the North Pacific/North American pattern illustrated in Fig. 2a, may be grouped into the following three categories.

a. The midlatitude atmosphere mainly responds to remote SST forcing in the tropical oceans

The potential role of tropical Pacific SST anomalies in modulating the intensity of the Aleutian low pressure center has been pointed out almost three decades ago in the pioneering work on ENSO by Bjerknes (1966, 1969). Interest in the "teleconnection" between the tropical ENSO phenomenon and the midlatitude atmospheric flow was revived in the early 1980s. Wallace and Gutzler (1981) compiled a thorough documentation of the most prevalent modes of wintertime atmospheric variability in the observed northern extratropics. The companion paper by Horel and Wallace (1981) pointed out that some of these atmospheric patterns are significantly correlated with ENSO-related SST changes in the tropical Pacific. The emergence of these empirical relationships coincided with a concerted effort by Rasmusson and Carpenter (1982), among others, to establish a firm observational basis of the tropical ENSO phenomenon.

Concurrent with the observational results cited above are advances in our theoretical understanding of the atmospheric dynamics that are pertinent to the link between tropical forcing and midlatitude response. By invoking the theory of energy dispersion developed by Rossby (1945) and Yeh (1949), Hoskins et al. (1977) demonstrated with a barotropic model that planetary-scale vorticity sources (as would be produced by latent heat release over the central equatorial Pacific due to enhanced precipitation in warm El Niño events) are capable of producing well-defined wave trains extending toward the extratropics. The horizontal shape of these model wave trains bears a considerable resemblance to observed anomaly patterns such as those shown in Fig. 2a. The atmospheric response to thermal forcing at various latitudes was further examined using a variety of barotropic and baroclinic models by Hoskins and Karoly (1981), Simmons (1982), Simmons et al. (1983), and Branstator (1985). These investigators reported that the forcing sites located in the Tropics or subtropics are most effective in generating a response in the middle and high latitudes. The results from these mechanistic models are clearly indicative of the driving of extratropical atmospheric anomalies by tropical heating sources.

The aforementioned empirical and theoretical works have been augmented by experimentation with comprehensive general circulation models (GCMs). Various investigators (e.g., Rowntree 1972; Blackmon et al. 1983; Shukla and Wallace 1983; among many others) have simulated the response of the model atmospheres to anomalous tropical Pacific SST conditions prescribed at the lower boundary. A majority of these studies was concerned with the long-term averaged model response to an idealized or observed tropical Pacific SST anomaly pattern, which is temporally fixed. An added degree of realism was built into the experimental design of the study by Lau (1985), in which the boundary forcing in the tropical Pacific was allowed to change with time in accordance with the observed month-to-month SST variations. The results from various GCM experiments generally confirm that the model atmospheres are indeed sensitive to SST conditions in the tropical Pacific and that the wintertime model response to these anomalies does appear in the form of a wave train in the North Pacific/North American sector.

The experiments examined in Lau (1985) were further diagnosed by Held et al. (1989) using a linearized version of the GCM, which is an effective tool for evaluating the relative importance of various processes in forcing the model atmosphere. The findings in the latter study indicate that the direct extratropical response to diabatic heating in the Tropics is actually rather weak. Instead, the extratropical atmosphere feels the impact of tropical heating indirectly through modification of the transient eddy forcing term by such heating. Held et al. further noted that the transient forcing could be associated with two processes: variations of the preferred trajectory of weather-scale midlatitude disturbances accompanying the perturbed extratropical wave train, and alterations in the spectrum of Rossby waves propagating from high to low latitudes due to anomalous zonal wind profiles in the Tropics. In light of these results, the scenario of the midlatitude wave train emanating directly from tropical heat sources, as put forth by Hoskins and Karoly (1981), has to be modified to include the vital role of transient disturbances.

b. The midlatitude atmospheric anomalies result mainly from in situ air–sea interactions in the extratropics

Long-range weather forecasters (e.g., Ratcliffe and Murray 1970; Namias 1975) have long been aware of certain well-defined spatial and temporal relationships between atmospheric and oceanic changes within the extratropics. Many of the earlier investigations on midlatitude air–sea interactions are concerned with the impact of SST anomalies on the atmosphere. However, the statistical study by Davis (1976) indicates that the correlations between SST and sea level pressure anomalies over the North Pacific are strongest when the atmospheric variations *lead* the oceanic changes by several months. This finding suggests that, contrary to the viewpoint held in the earlier works, extratropical air–sea coupling mainly entails the driving of the ocean by the overlying atmosphere.

Research on extratropical air–sea interactions received a new boost from the modeling and observational study of Palmer and Sun (1985). These authors demonstrated that an atmospheric GCM is capable of generating a realistic response when forced by SST anomalies in the northwestern Atlantic. Our observational knowledge of the preferred modes of extratropical atmosphere–ocean variability is also enhanced due to the systematic documentations by Wallace and Jiang (1987) and Wallace et al. (1990). These studies illustrate that prominent atmospheric teleconnection patterns in the Pacific/North American and western Atlantic sectors are strongly correlated with well-defined SST anomaly patterns in the North Pacific and North Atlantic, respectively. They also confirm the earlier finding by Davis (1976) that perturbations in the atmosphere occur prior to those in the ocean.

Additional GCM integrations conducted by Pitcher et al. (1988), Kushnir and Lau (1992), Peng et al. (1995), and Kushnir and Held (1996), among others, also indicated some model sensitivity to SST anomalies prescribed in the North Pacific and North Atlantic. However, the simulated responses to midlatitude SST changes are generally not as reproducible as the responses to tropical SST forcing. In particular, influences of extratropical SST changes on the model atmosphere appear to be dependent on details of model numerics and physics, experimental design, timescale, initial atmospheric conditions, configuration of the climatological background flow, as well as spatial structure of the SST anomaly. Another perplexing issue with these modeling studies is that the atmospheric response exhibits a notable degree of nonlinearity with respect to the polarity of the prescribed SST forcing; that is, the atmospheric signal does not simply undergo a sign reversal when a warm anomaly is replaced by a cold anomaly. Attempts to generate a robust response to midlatitude SST anomalies have met with relatively more success by using GCMs with higher spatial resolution, as have been demonstrated by the experiments of Latif and Barnett (1994) and Ferranti et al. (1994).

In summary, a full understanding of the nature of feedback processes participating in midlatitude air–sea interaction is still lacking. Moreover, if the extratropical coupling is indeed dominated by the atmosphere driving the ocean, as some of the lag correlation statistics seem to indicate, questions concerning the origin of the atmospheric anomalies responsible for generating oceanic changes remain unanswered.

c. *Low-frequency atmospheric anomalies in midlatitudes are mainly manifestations of internal dynamical processes*

This class of hypotheses is based on the premise that, even in the absence of external forcing mechanisms such as SST changes, low-frequency meteorological features can occur as a result of processes operating within the atmosphere itself. The myriad internal mechanisms that could potentially contribute to atmospheric fluctuations on long timescales have been reviewed by Wallace and Blackmon (1983).

In recent years, considerable attention has been devoted to the mutual interactions between low-frequency anomalies and aggregates of active weather-scale fluctuations (often referred to as "storm tracks"). Observational evidence presented by Lau (1988), Metz (1989), and many others demonstrates that a close relationship exists between the variability of the large-scale flow pattern and the location or intensity of the storm tracks. The planetary wave structure is associated with zones of enhanced baroclinicity and horizontal wind shear, which are preferred sites for the genesis and intensification of fast-moving disturbances. The latter fluctuations, once generated, tend to reinforce any preexistent perturbation in the background flow, mainly through eddy transports of vorticity in the upper troposphere. In this manner, anomalies in the large-scale flow may be maintained by transient disturbances embedded in the storm tracks.

The broader issue of whether internal processes alone may generate realistic amplitudes and spatial patterns of atmospheric variability was addressed by Manabe and Hahn (1981) and Lau (1981) using output from a 15-yr GCM integration. Climatological SST conditions were prescribed in the world's oceans throughout the course of this experiment so that no interannual variability was introduced at the lower boundary of the model atmosphere. Analysis of the model data indicates that not only does the extratropical atmosphere exhibit a considerable level of "natural" variability on monthly and seasonal timescales, the principal spatial modes of the simulated fluctuations also bear some resemblance to their observed counterparts. Comparison between the simulations with and without prescribed SST anomalies (e.g., see Lau 1985) reveals that the temporal variability of the midlatitude atmosphere is not noticeably enhanced in the presence of SST fluctuations. We can infer from these GCM results that a substantial fraction of the atmospheric variance may be attributed to dynamical mechanisms not related to any boundary forcing.

It should be noted that the anomalies generated within the atmosphere could in turn interact with the underlying ocean and thereby incite variability of the coupled air–sea system. This notion is supported by the recent results of Delworth (1996) and Bladé (1996, submitted to *J. Climate*), who examined the extratropical variability simulated by coupled GCMs in the absence of ENSO-related tropical SST forcing. These authors reported that coupled variability in midlatitudes is largely the result of the surface ocean responding to anomalous heat fluxes induced by internally generated atmospheric modes. I. Bladé (1996, submitted to *J. Climate*) also pointed out that the persistence of the atmospheric anomalies as well as the 850-hPa temperature variance at low frequencies are increased in the presence of air–sea coupling. It is evident from these modeling studies that the internal atmospheric processes discussed in the present subsection could play a substantial role in the extratropical coupled atmosphere–ocean phenomena described in the previous subsection. The linkage between the mechanisms considered in these two sections would be particularly strong if positive feedbacks exist among the internally produced atmospheric fluctuations and the corresponding oceanic changes.

4. Systematic assessment of the impact of various SST forcing scenarios and internal dynamics

a. Experimental design

To evaluate the relative importance of the various mechanisms discussed in the previous section, an extensive series of experiments has been conducted using the same global climate GCM developed and maintained at GFDL. Horizontal variations in this model atmosphere are represented spectrally with a rhomboidal truncation at 15 wavenumbers. Vertical variations are computed at nine sigma levels. Realistic land–sea contrast and orography are prescribed at the lower boundary. A comprehensive set of physical processes is incorporated in this model, including a full hydrological cycle, radiative transfer, variable cloud cover, and sea ice formation. Further details of the model formulation can be found in Gordon and Stern (1982). Altogether five experiments have been conducted.

- The 100-yr "control" experiment, in which climatological SST data are prescribed at all ocean grid points, so that the maritime lower boundary is constrained to evolve through identical annual cycles.
- The Global Ocean–Global Atmosphere (GOGA) experiment, in which the SST conditions at all ocean grid points between 40°S and 60°N are continuously updated using the monthly observations for the 1946–88 period. The climatological seasonal cycle of SST (with no interannual variations) is prescribed elsewhere in the world's oceans.
- The Tropical Ocean–Global Atmosphere (TOGA) experiment, which is similar to the GOGA experiment, except that the observed month-to-month SST variations are inserted only at grid points in the tropical Pacific between 25°S and 25°N.
- The Midlatitude Ocean–Global Atmosphere (MOGA) experiment, which is similar to the GOGA experiment, except that the observed variable SST forcing is prescribed only in the North Pacific between 25° and 55°N.
- The Tropical Ocean–Global Atmosphere Mixed Layer (TOGA–ML) experiment, which is similar to the TOGA experiment, except that the SST anomalies outside the tropical Pacific are predicted using an oceanic mixed layer model. Specifics of the mixed layer model as well as the conclusions drawn from this experiment will be discussed in section 5.

The schematic diagram in Fig. 3 illustrates the respective oceanic domains in which time-varying and climatological SST forcings are prescribed or predicted in the last four experiments in the above list. For each of the GOGA, TOGA, MOGA, and TOGA–ML experiments, an ensemble of four independent integrations is performed, with each integration being initiated from a different set of atmospheric conditions but subjected to the same scenario of SST forcing during 1946–88. The larger sample size provided by such multiple runs allows for a more reliable assessment of the reproducibility and statistical significance of the model responses. For a given SST scenario, the results from the four independent integrations are averaged for individual years. We shall henceforth refer to these averages as the "four-run ensemble means." More elaborate analyses of the 100-yr con-

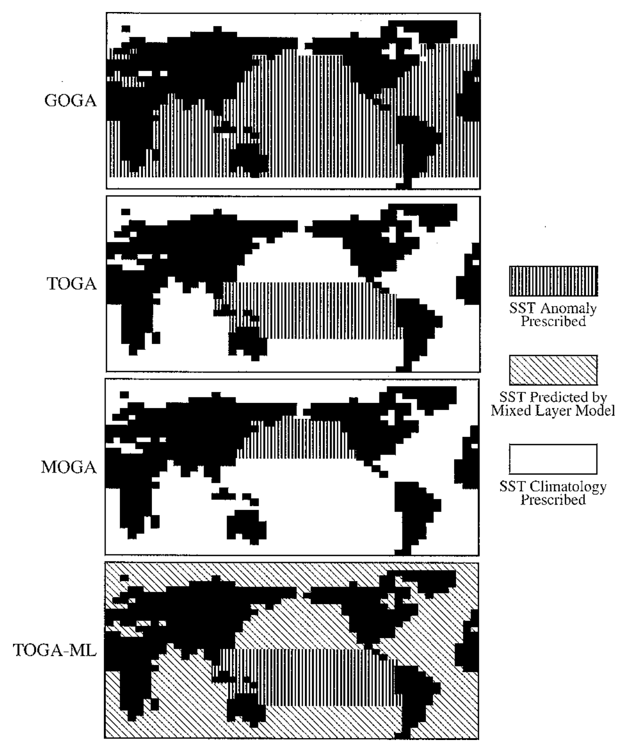

FIG. 3. Schematic diagram depicting treatment of the oceanic boundary conditions in the GOGA, TOGA, MOGA, and TOGA-ML experiments.

trol run are reported in Ting and Lau (1993). Results from the GOGA, TOGA, and MOGA experiments are described in greater detail in Lau and Nath (1994). Findings based on TOGA–ML are presented in Lau and Nath (1996).

b. Results

To compare the spatial pattern and amplitude of the model response to SST anomalies prescribed at different geographical sites, we have analyzed the model output using the same composite procedure developed in section 2 for the observations. For a given experiment, an average is taken of the four-run ensemble means over the set of seven WTP/CNP winters, and another average is taken over the seven CTP/WNP winters. The differences between these two averages (WTP/CNP–CTP/WNP) for 515-hPa height in the (a) GOGA, (b) TOGA, and (c) MOGA experiments are presented in Fig. 4. Comparison of the three model patterns with each other, and with their observed counterpart in Fig. 2a, reveals that a strong degree of resemblance exists between the GOGA and TOGA simulations, as well as between these two runs and the observations. On the other hand, the anomalies generated in the MOGA experiments are weaker than those in GOGA and TOGA and do not exhibit any spatial correspondence with the GOGA, TOGA, and observational results.

The evidence presented in Figs. 4 and 2a indicates that the model atmosphere is capable of generating a realistic response pattern when it is forced with near-global SST anomalies, as is done in the GOGA runs. However, the same response pattern can be simulated by prescribing the tropical Pacific SST forcing alone in the TOGA experiment, thus implying that a substantial portion of the GOGA signal can be attributed to ENSO-related SST fluctuations in the tropical Pacific. The feeble response in the MOGA experiment illustrates the less significant role of midlatitude SST anomalies in altering the overlying atmospheric circulation. Similar conclusions have been drawn by Graham et al. (1994) and Ferranti et al. (1994) on the basis of GCM experiments analogous to those described here. The findings from these independent investigations affirm that remote forcing by tropical heat sources exert a more noticeable impact on the extratropical atmosphere than local forcing by midlatitude SST anomalies.

Although the GOGA and TOGA runs have considerable success in reproducing the qualitative features in the observed height anomaly pattern, the amplitude of the composite model responses is typically weaker than the observed values by a factor of 2–3. This notable discrepancy between model and observations could result from several factors. The spatial resolution of the GCM used for this series of experiments might be too low to simulate the full impact of transient eddy forcing in both the Tropics and extratropics, which are known to contribute significantly to the quasistationary response (see discussion in sections 3a and 3c). Second, the low-latitude condensational heating as simulated by this GCM in response to tropical SST anomalies is noticeably weaker than that inferred from observations. This reduction in the intensity of the heat sources and sinks in the model Tropics would in

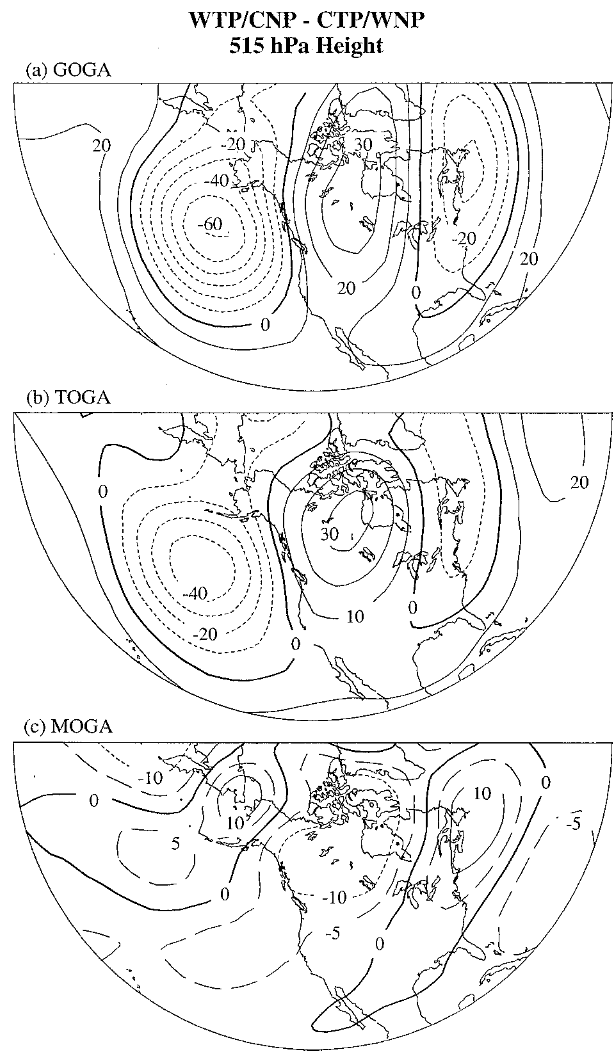

FIG. 4. As in Fig. 2a but for 515-hPa height data simulated in the (a) GOGA, (b) TOGA, and (c) MOGA experiments. Contour interval: 10 m. Contours with long dashes in (c) indicate values of ±5m.

turn lead to diminished teleconnections with the extratropics. Last, the model results in Fig. 4 are based on averages over four different realizations of the model atmosphere for a given sequence of SST boundary conditions, whereas only a single realization is available from the observational records for constructing the pattern in Fig. 2a. Due to the presence of sampling fluctuations among the four independent model runs, the amplitude of the four-run ensemble mean is typically weaker than that simulated in individual integrations.

The relatively weak model response to North Pacific SST anomalies in the MOGA experiment (Fig. 4c) should be viewed in the context of the coarse resolution of the GCM being used, as well as the experimental design of the current series of model runs. As has been noted in section 3b, integrations of models with higher resolution (e.g., Latif and Barnett 1994) have yielded stronger responses to extratropical SST forcing. Such stronger signals could in part be attributed to the simulation of more vigorous storm tracks and eddy-mean flow interactions in high-resolution models. Moreover, the investigations of Palmer and Sun (1985), among others, indicate that midlatitude air–sea coupling is sensitive to the spatial relationship between the SST anomaly and the storm tracks. In the MOGA runs, *observed* extratropical SST anomalies have been inserted in a *model-simulated* environment that contains systematic errors in the location of the storm tracks. It is unlikely that this experimental setup would achieve an "optimal" degree of coupling between the atmosphere and ocean. One would hence anticipate that the atmospheric response to extratropical SST anomalies is underestimated in the MOGA experiment.

We now turn our attention to the simulation by the 100-yr control experiment. Since this integration has been conducted in the absence of any time-varying SST forcing at the lower boundary, its output should provide useful information on the contribution of internal dynamical processes to the characteristic anomaly patterns appearing in GOGA, TOGA, and the observations. In order to identify the recurrent anomaly patterns in the control experiment, we have performed a principal component (PC) analysis (e.g., see Kutzbach 1967) of the northern winter means of the 515-hPa height field from this model run.

Inspection of the leading spatial modes obtained from the PC analysis reveals that the control experiment is indeed capable of generating a characteristic pattern similar to that identified in the model runs forced by SST variations. This particular PC in the control run explains 17% of the domain-integrated variance. Its spatial structure may be discerned by compositing the model output according to the time series of expansion coefficients associated with the PC of interest. For a given PC, the magnitude and sign of the expansion coefficient for a given winter provides a measure of the spatial similarity and polarity of the anomaly pattern in that winter with respect to the PC in question. In analogy with the method used in constructing the patterns in Figs. 2 and 4, the compositing procedure entails the averaging over 16 winters with the most positive expansion coefficients, and over 16 winters with the most negative expansion coefficients, and taking the difference between the two averages. The rationale for using 16 winters to compute the composite pattern for a given polarity is that they constitute about one-sixth of the data sample. A similar fraction (i.e., seven WTP/CNP or CTP/WNP winters in the 42-winter period of 1946–88) has been used in constructing the composites in Figs. 2a and 4.

Application of the composite procedure based on PC coefficients yields Fig. 5 for the 515-hPa height field in the control run. This pattern resembles the observed and simulated anomalies related to SST changes (see Figs. 2a and 4a,b). The presence of this characteristic pattern in the control run signifies that internal dynamics makes substantial contributions to the low-frequency variability of the midlatitude atmosphere. The insertion of time-varying boundary forcing in the GOGA and TOGA runs apparently enhances the frequency of occurrence of such internal atmospheric modes during the prominent SST epi-

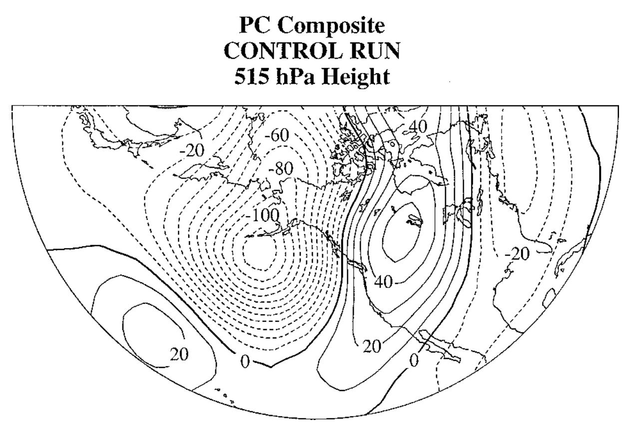

Fig. 5. As in Fig. 4 but for data simulated in the control experiment. The pattern depicts the difference between the average of 16 winters with the largest positive temporal coefficients for a selected principal component and the average of 16 winters with the largest negative coefficients.

sodes, thus resulting in model responses (see Figs. 4a,b) that exhibit considerable similarity with one of the preferred anomaly patterns in the control experiment (Fig. 5).

5. The atmospheric bridge linking tropical Pacific ENSO events to SST variability in the North Pacific

To search for an explanation for the coincidence of SST changes in the tropical Pacific with oceanic anomalies in the midlatitude North Pacific (see Fig. 2b and the second question raised at the end of section 2), we first examine the impact of the extratropical atmospheric anomaly generated by tropical Pacific SST forcing in TOGA on the underlying ocean. The WTP/CNP–CTP/WNP composite patterns of wintertime sea level pressure (contours) and the sum of ocean-to-atmosphere latent and sensible heat fluxes (stippling) as computed using the four-run ensemble averages of the TOGA output, are displayed in Fig. 6. For the sake of brevity, the following discussion pertains to model responses to warm tropical Pacific SST forcing. The polarity of the anomalies described below needs to be reversed while considering responses to cold tropical SST anomalies. The most prominent response of the near-surface atmospheric flow takes the form of a deepened Aleutian low, which lies below the negative 515-hPa height anomaly at the same location (see Fig. 4b). This low pressure anomaly is accompanied by an enhanced cyclonic circulation in the North Pacific, with intensified northerly surface flow to the west of the low center, westerly flow in the central Pacific between 30° and 40°N, and southerly flow to the east of the low.

Bearing in mind that both temperature and specific humidity generally decrease from low to high latitudes, the strengthening of northerly flow in the Northern Hemisphere would result in anomalous advection of cool and dry air over the ocean surface, whereas southerly flow anomalies would have the opposite effect. The superposition of eastward flow anomalies on the midlatitude climatological westerly wind belt in the central Pacific would lead to increased wind speeds in that region. The latent and sensible heat exchange across the air–sea interface are related by bulk aerodynamic laws to the surface wind speed and the local air–sea gradients of humidity and temperature. The perturbations in the latter atmospheric variables caused by the cyclonic anomaly in the North Pacific would reduce the heat loss from the ocean to the atmosphere (thus resulting in oceanic warming) in the region east of the anomalous low center and enhance the heat loss (oceanic cooling) in regions south and west of this center. This chain of arguments is consistent with the spatial relationships between the heat flux and sea level pressure anomaly patterns in Fig. 6 and with the observational evidence presented by Cayan (1992a,b). The composite heat flux data presented in this figure (stippling) portray the atmospheric driving of the North Pacific waters resulting from the remote meteorological response to SST variations prescribed in the ENSO region. Comparison between this *TOGA-simulated* heat flux anomaly pattern with the *observed* SST changes in the North Pacific for the same set of winters (see Fig. 2b) reveals that positive anomalies in ocean-to-atmosphere heat flux are collocated with cold SST anomalies, and vice versa. This remarkable spatial correspondence between the two fields offers strong indication that fluctuations in the North Pacific SST are caused by variability in the overlying atmosphere, which in turn originates from oceanic forcing in the tropical Pacific.

A schematic representation of the processes linking the air–sea coupled system in different latitudes is given in Fig. 7. This diagram highlights the primary

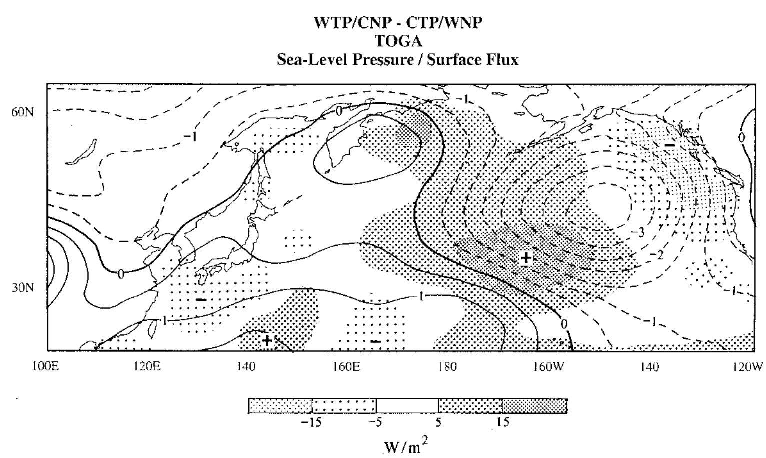

FIG. 6. Composite patterns obtained by subtracting the average over the seven CTP/WNP winters from the average over the seven WTP/CNP winters for sea level pressure (contours, interval: 0.5 hPa) and ocean-to-atmosphere latent and sensible heat flux (stippling, see scale bar at bottom, units: W m^{-2}) as simulated in the TOGA experiment.

role of ENSO episodes in setting the pace for ocean–atmosphere variability in the entire Pacific basin, with the atmospheric circulation serving as a "bridge" between oceanic anomalies in the tropical sector and those in the extratropics. Also illustrated in Fig. 7 are the intimate relationships between the storm tracks and quasistationary waves in the extratropics (as pointed out in section 3c), both of which could influence (and in turn be influenced by) the local oceanic conditions. Understanding of the three-way interactions among the planetary-scale waves, weather-scale disturbances traveling along the storm tracks, and the extratropical SST perturbations is therefore a critical component in any research program on air–sea coupling in midlatitudes.

We proceed to test the validity of the atmospheric bridge hypothesis by actually allowing the atmospheric response generated in TOGA to force SST changes in ocean sites lying beyond the tropical Pacific. The TOGA–ML experiment mentioned in section 4a (see also last panel in Fig. 3) is conducted with this purpose in mind. The main difference between the TOGA and TOGA–ML runs is that a simple mixed layer model of the surface ocean is incorporated in the latter experiment at ocean grid points situated outside of the tropical Pacific. The mixed layer model used is a motionless, one-dimensional column of water with a constant depth of 50 m. No interaction is permitted between neighboring columns, or between each column and the deep ocean lying below. The temperature fluctuations in this mixed layer are solely determined by the variability of the heat fluxes at the air–sea interface, which is in turn related to changes in atmospheric temperature, humidity, and wind speed at the ocean surface. By coupling the mixed layer model to the atmospheric GCM, the atmospheric variables are also allowed to respond to changes in the mixed layer temperature. The TOGA–ML experiment hence incorporates a simple form of two-way ocean–atmosphere interaction at maritime locations beyond the tropical Pacific. As in the TOGA experiment, altogether four independent TOGA–ML runs are conducted for the 1946–88 period.

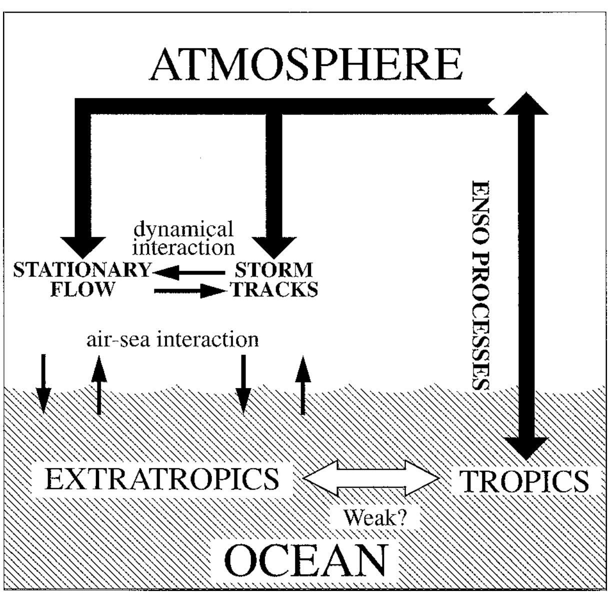

FIG. 7. Schematic diagram depicting the role of the atmospheric bridge in linking SST variations in the tropical and extratropical oceans.

The WTP/CNP–CTP/WNP composite for the four-run ensemble mean of the mixed layer temperature computed in the TOGA–ML experiment in the extratropical North Pacific is shown in Fig. 8. Comparison of this model result with its observed counterpart (Fig. 2b) reveals many similarities, thus confirming that the simulated atmospheric response to tropical Pacific SST anomalies is capable of driving realistic oceanic changes in the North Pacific. Alexander (1992), Luksch and von Storch (1992), and Miller et al. (1994) have analyzed model experiments analogous to the TOGA–ML run. Their findings also support a role for the atmosphere as a link between SST anomalies in the tropical Pacific and those in the North Pacific.

The amplitude of the simulated mixed layer temperature variations in the TOGA–ML experiment is typically lower than the observed values by a factor of 2. This result is evidently related to the weaker atmospheric responses to tropical SST forcing in the model atmosphere (Fig. 4b) as compared to observations (Fig. 2a). As can be expected, a good spatial correspondence also exists between the pattern of anomalous heat fluxes in TOGA (stippling in Fig. 6) and that of mixed layer temperature in TOGA–ML (Fig. 8).

We now consider the impact on the atmosphere of two-way air–sea interactions operating in the TOGA–ML experiment. The WTP/CNP–CTP/WNP composite of the 515-hPa height field based on the four-run ensemble means of TOGA–ML output is presented in Fig. 9. This pattern exhibits a notable resemblance to the corresponding result from the TOGA runs (Fig. 4b), which are performed in the absence of any SST variability beyond the tropical Pacific. The amplitude of the height anomalies generated in TOGA–ML is typically stronger than the TOGA response by

30%. The enhancement of the atmospheric signal in the TOGA–ML scenario suggests that the mixed layer temperature changes driven by a given atmospheric perturbation tend to reinforce the same atmospheric anomaly, thus setting up a positive feedback loop linking the oceanic and atmospheric fluctuations. A similar air–sea feedback in the North Pacific is also evident in the coupled experiments conducted by Gallimore (1995). The nature of the processes participating in the feedback chain remains to be ascertained. It is likely that, as is indicated in the schematic diagram shown in Fig. 7, the transient features along the oceanic storm tracks could play an important role in this feedback.

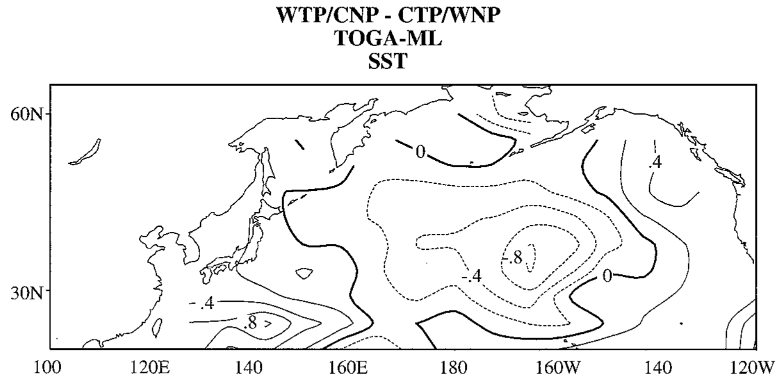

FIG. 8. As in Fig. 6 but for mixed layer temperature simulated in the TOGA–ML experiment. Contour interval: 0.2°C.

6. Discussion

By making use of long-term observational data records, extensive experimentation with numerical models of various degrees of sophistication, and guidance from theoretical studies, we are gradually unraveling the complex interactions between the atmosphere and ocean in different geographical settings. It is anticipated that the inferences drawn from the multitude of modeling investigations conducted thus far will be refined and sharpened as integrations using GCMs with improved physical parameterizations and spatial resolution become feasible. In particular, some of the outstanding issues concerning extratropical air–sea interaction could be resolved by experimentation with models that provide more realistic simulations of the storm track eddies and the transfer processes in the atmospheric and oceanic boundary layers.

The availability of ever-increasing computing resources has facilitated the implementation of multiple model runs with very long durations, such as the 43-yr SST runs and the 100-yr control run described here. These extended integrations allow for more comprehensive diagnoses of the commonalities and distinctions among the prominent anomalous SST episodes occurring in the historical record. The long-term simulations also provide opportunities to examine the nature of atmospheric variability on the decadal timescale. An example of such low-frequency phenomena is the prolonged period of warm tropical Pacific anomalies and cold North Pacific anomalies in the SST records for the late 1970s and much of the 1980s (see Fig. 1 of this paper, and the review by Trenberth 1990). Deser and Blackmon (1995) further noted that the cooling trend in the North Pacific during 1950–87 is linearly independent of SST variability in the tropical Pacific. The origin of such decadal variations remains to be fully understood. The relative roles of the ocean and atmosphere in the formation and maintenance of these decadal anomalies could well be different from those described in the present article, which is focused on ENSO-related fluctuations with typical timescales of 2–4 yr. For instance, the empirical evidence presented by Deser and Blackmon (1993) and Kushnir (1994) suggests that the ocean circulation could become a more active participant in coupled variability on the decadal timescale, whereas the oceanic response to atmospheric driving is the primary factor in midlatitude air–sea interactions on seasonal and annual timescales. Simulation of the interdecadal

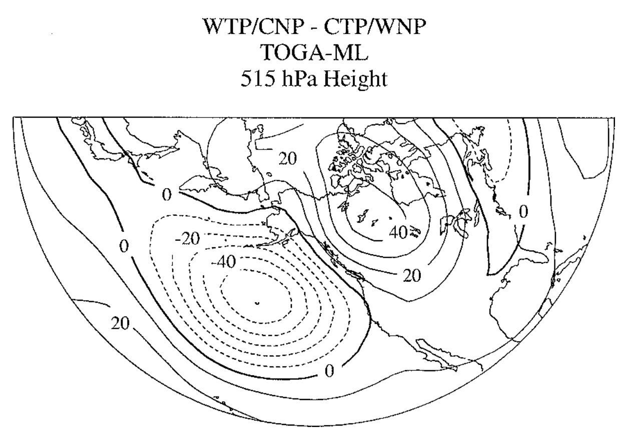

FIG. 9. As in Fig. 4 but for data simulated in the TOGA–ML experiment.

variability of the climate system would ultimately have to be conducted with comprehensive ocean–atmosphere coupled GCMs.

Acknowledgments. The results based on the GFDL GCM as presented here are the fruit of many years of interactions with colleagues at GFDL and other institutions. I am indebted to these collaborators (who are too numerous to mention individually) for generously sharing with me their insights on different facets of air–sea coupling. I wish to specifically thank Mary Jo Nath of GFDL for having tirelessly assisted me in conducting and analyzing the large number of model integrations during the past decade. The constructive comments by the three official reviewers (Yochanan Kushnir, Tim N. Palmer, and John M. Wallace) have been helpful in clarifying some of the issues addressed here. Part of this research effort has been supported by the NOAA Climate and Global Change Program.

This review is a modified version of a contribution to the monograph *From Atmospheric Circulation to Global Change* (ISBN 7-5029-2098-6), which was published in 1996 in celebration of the 80th birthday of Professor Ye Duzheng (T.-C. Yeh), an honorary member of the American Meteorological Society. A brief biography of Professor Ye can be found on pages 928–929 of the June 1991 issue of the *Bulletin of the American Meteorological Society.* Permission of the China Meteorological Press to publish this article in its present form is gratefully acknowledged.

References

Alexander, M. A., 1992: Midlatitude atmosphere–ocean interaction during El Niño. Part I: The North Pacific Ocean. *J. Climate,* **5,** 944–958.

Bjerknes, J., 1966: A possible response of the atmosphere Hadley circulation to equatorial anomalies of ocean temperature. *Tellus,* **18,** 820–829.

——, 1969: Atmospheric teleconnections from the equatorial Pacific. *Mon. Wea. Rev.,* **97,** 163–172.

Blackmon, M. L., J. E. Geisler, and E. J. Pitcher, 1983: A general circulation model study of January climate anomaly patterns associated with interannual variation of equatorial Pacific sea surface temperatures. *J. Atmos Sci.,* **40,** 1410–1425.

Branstator, G., 1985: Analysis of general circulation model sea-surface temperature anomaly simulations using a linear model. Part I: Forced solutions. *J. Atmos. Sci.,* **42,** 2225–2241.

Cayan, D. R., 1992a: Latent and sensible heat flux anomalies over the northern oceans: The connection to monthly atmospheric circulation. *J. Climate,* **5,** 354–369.

——, 1992b: Latent and sensible heat flux anomalies over the northern oceans: Driving the sea surface temperature. *J. Phys. Oceanogr.,* **22,** 859–881.

Davis, R. E., 1976: Predictability of sea surface temperature and sea level pressure anomalies over the North Pacific Ocean. *J. Phys. Oceanogr.,* **6,** 249–266.

Delworth, T. L., 1996: North Atlantic interannual variability in a coupled ocean–atmosphere model. *J. Climate,* **9,** 2356–2375.

Deser, C., and M. L. Blackmon, 1993: Surface climate variations over the North Atlantic Ocean during winter: 1900–1989. *J. Climate,* **6,** 1743–1753.

——, and ——, 1995: On the relationship between tropical and North Pacific sea surface temperature variations. *J. Climate,* **8,** 1677–1680.

Ferranti, L., F. Molteni, and T. N. Palmer, 1994: Impact of localized tropical and extratropical SST anomalies in ensembles of seasonal GCM integrations. *Quart. J. Roy. Meteor. Soc.,* **120,** 1613–1645.

Folland, C. K., and D. E. Parker, 1990: Observed variations of sea surface temperature. *Climate–Ocean Interaction,* M. E. Schlesinger, Ed., Kluwer, 21–52.

Gallimore, R. G., 1995: Simulated ocean–atmosphere interaction in the North Pacific from a GCM coupled to a constant-depth mixed layer. *J. Climate,* **8,** 1721–1737.

Gordon, C. T., and W. F. Stern, 1982: A description of the GFDL global spectral model. *Mon. Wea. Rev.,* **110,** 625–644.

Graham, N. E., T. P. Barnett, R. Wilde, U. Schlese, and L. Bengtsson, 1994: On the roles of tropical and midlatitude SSTs in forcing interannual to interdecadal variability in the winter Northern Hemisphere circulation. *J. Climate,* **7,** 1416–1441.

Held, I. M., S. W. Lyons, and S. Nigam, 1989: Transients and the extratropical response to El Niño. *J. Atmos. Sci.,* **46,** 163–174.

Horel, J. D., and J. M. Wallace, 1981: Planetary scale atmospheric phenomena associated with the Southern Oscillation. *Mon. Wea. Rev.,* **109,** 813–829.

Hoskins, B. J., and D. J. Karoly, 1981: The steady linear response of a spherical atmosphere to thermal and orographic forcing. *J. Atmos. Sci.,* **38,** 1179–1196.

——, A. J. Simmons, and D. G. Andrews, 1977: Energy dispersion in a barotropic atmosphere. *Quart. J. Roy. Meteor. Soc.,* **103,** 553–567.

Hsiung, J., and R. E. Newell, 1983: The principal nonseasonal modes of variation of global sea surface temperature. *J. Phys. Oceanogr.,* **13,** 1957–1967.

Kushnir, Y., 1994: Interdecadal variations in North Atlantic sea surface temperature and associated atmospheric conditions. *J. Climate,* **7,** 141–157.

——, and N.-C. Lau, 1992: The general circulation model response to a North Pacific SST anomaly: Dependence on time scale and pattern polarity. *J. Climate,* **5,** 271–283.

——, and I. M. Held, 1996: On the equilibrium response to North Atlantic SST anomalies. *J. Climate,* **9,** 1208–1220.

Kutzbach, J. E., 1967: Empirical eigenvectors of sea-level pressure, surface temperature and precipitation complexes over North America. *J. Appl. Meteor.,* **6,** 791–802.

Latif, M., and T. P. Barnett, 1994: Causes of decadal climate variability over the North Pacific and North America. *Science,* **266,** 634–637.

Lau, N.-C., 1981: A diagnostic study of recurrent meteorological anomalies appearing in a 15-year simulation with a GFDL general circulation model. *Mon. Wea. Rev.,* **109,** 2287–2311.

——, 1985: Modeling the seasonal dependence of the atmospheric response to observed El Niños in 1962–76. *Mon. Wea. Rev.,* **113,** 1970–1996.

——, 1988: Variability of the observed midlatitude storm tracks in relation to low-frequency changes in the circulation pattern. *J. Atmos. Sci.,* **45,** 2718–2743.

——, and M. J. Nath, 1994: A modeling study of the relative roles of tropical and extratropical SST anomalies in the variability of the global atmosphere–ocean system. *J. Climate,* **7,** 1184–1207.

——, and ——, 1996: The role of the "atmospheric bridge" in linking tropical Pacific ENSO events to extratopical SST anomalies. *J. Climate,* **9,** 2036–2057.

Luksch, U., and H. von Storch, 1992: Modeling the low-frequency sea surface temperature variability in the North Pacific. *J. Climate,* **5,** 893–906.

Manabe, S., and D. G. Hahn, 1981: Simulation of atmospheric variability. *Mon. Wea. Rev.,* **109,** 2260–2286.

Metz, W., 1989: Low-frequency anomalies of atmospheric flow and effects of cyclone-scale eddies: A canonical correlation analysis. *J. Atmos. Sci.,* **46,** 1026–1041.

Miller, A. J., D. R. Cayan, T. P. Barnett, N. E. Graham, and J. J. Oberhuber, 1994: Interdecadal variability of the Pacific Ocean: Model response to observed heat flux and wind stress anomalies. *Climate Dyn.,* **9,** 287–302.

Namias, J., 1969: Seasonal interactions between the North Pacific Ocean and the atmosphere during the 1960's. *Mon. Wea. Rev.,* **97,** 173–192.

——, 1975: *Short Period Climatic Variations. Collected Works of J. Namias, 1934 through 1974.* Vols. I and II. University of California, San Diego, 905 pp.

Nitta, T., and S. Yamada, 1989: Recent warming of tropical sea surface temperature and its relationship to the Northern Hemisphere circulation. *J. Meteor. Soc. Japan,* **67,** 375–383.

Palmer, T. N., and Z.-B. Sun, 1985: A modelling and observational study of the relationship between sea surface temperature in the north-west Atlantic and the atmospheric general circulation. *Quart. J. Roy. Meteor. Soc.,* **111,** 947–975.

Pan, Y. H., and A. H. Oort, 1990: Correlation analyses between sea surface temperature anomalies in the eastern equatorial Pacific and the World Ocean. *Climate Dyn.,* **4,** 191–205.

Peng, S., L. A. Mysak, H. Ritchie, J. Derome, and B. Dugas, 1995: The difference between early and midwinter atmospheric responses to sea surface temperature anomalies in the northwest Atlantic. *J. Climate,* **8,** 137–157.

Pitcher, E. J., M. L. Blackmon, G. T. Bates, and S. Muñoz, 1988: The effect of North Pacific sea surface temperature anomalies on the January climate of a general circulation model. *J. Atmos. Sci.,* **45,** 173–188.

Rasmusson, E. M., and T. H. Carpenter, 1982: Variations in tropical sea surface temperature and surface wind fields associated with the Southern Oscillation/El Niño. *Mon. Wea. Rev.,* **110,** 354–384.

Ratcliffe, R. A. S., and R. Murray, 1970: New lag associations between North Atlantic sea temperature and European pressure applied to long-range weather forecasting. *Quart. J. Roy. Meteor. Soc.,* **96,** 226–246.

Rossby, C.-G., 1945: On the propagation of frequencies and energy in certain types of oceanic and atmospheric waves. *J. Meteor.,* **2,** 187–203.

Rowntree, P. R., 1972: The influence of tropical east Pacific Ocean temperatures on the atmosphere. *Quart. J. Roy. Meteor. Soc.,* **98,** 290–321.

Shukla, J., and J. M. Wallace, 1983: Numerical simulation of the atmospheric response to equatorial Pacific sea surface temperature anomalies. *J. Atmos. Sci.,* **40,** 1613–1630.

Simmons, A. J., 1982: The forcing of stationary wave motion by tropical diabatic heating. *Quart. J. Roy. Meteor. Soc.,* **108,** 503–534.

——, J. M. Wallace, and G. W. Branstator, 1983: Barotropic wave propagation and instability, and atmospheric teleconnection patterns. *J. Atmos. Sci.,* **40,** 1363–1392.

Ting, M., and N.-C. Lau, 1993: A diagnostic and modeling study of the monthly mean wintertime anomalies appearing in a 100-year GCM experiment. *J. Atmos. Sci.,* **50,** 2845–2867.

Trenberth, K. E., 1990: Recent observed interdecadal climate changes in the Northern Hemisphere. *Bull. Amer. Meteor. Soc.,* **71,** 988–993.

van Loon, H., and R. A. Madden, 1981: The Southern Oscillation. Part I: Global associations with pressure and temperature in northern winter. *Mon. Wea. Rev.,* **109,** 1150–1162.

Wallace, J. M., and D. S. Gutzler, 1981: Teleconnections in the geopotential height field during the Northern Hemisphere winter. *Mon. Wea. Rev.,* **109,** 784–812.

——, and M. L. Blackmon, 1983: Observations of low-frequency atmospheric variability. *Large-Scale Dynamical Processes in the Atmosphere,* B. J. Hoskins and R. P. Pearce, Eds., Academic Press, 55–94.

——, and Q.-R. Jiang, 1987: On the observed structure of the interannual variability of the atmosphere/ocean climate system. *Atmospheric and Oceanic Variability,* H. Cattle, Ed., Roy. Meteor. Soc., 17–43.

——, C. Smith, and Q.-R. Jiang, 1990: Spatial patterns of atmosphere/ocean interaction in the northern winter. *J. Climate,* **3,** 990–998.

Weare, B. C., A. Navato, and R. E. Newell, 1976: Empirical orthogonal analysis of Pacific Ocean sea surface temperatures. *J. Phys. Oceanogr.,* **6,** 671–678.

Yeh, T.-C., 1949: On energy dispersion in the atmosphere. *J. Meteor.,* **6,** 1–16.